RSC Advances

PAPER

View Article Online
View Journal | View Issue

Cite this: *RSC Adv.*, 2017, **7**, 26770

Special properties of luminescent magnetic $NaGdF_4$:Yb^{3+}, Er^{3+} upconversion nanocubes with surface modifications†

Longyi Chen,[a] Wai Hei Tse,[b] Alex Siemiarczuk[c] and Jin Zhang *[ab]

Received 22nd March 2017
Accepted 9th May 2017

DOI: 10.1039/c7ra03380j

rsc.li/rsc-advances

A one-pot process is developed to produce $NaGdF_4$:Yb^{3+}, Er3+ upconversion nanocubes (UCNCs) with amine surface modifications. The photoluminescence and magnetic properties of the amine modified unpconversion nanocubes (UCNCs) were investigated. The emissions of green light at 540 nm and red light at 660 nm are observed under infrared excitation (λ_{ex} = 980 nm) to both of UCNCs in aqueous solution and dry form. The emission at 660 nm is inhibited by non-radiative decay process when water interacts with the amine functional group on the surface of nanocubes. In addition, the magnetic susceptibility of the nanocubes is 1.049×10^{-4} emu g^{-1} Oe^{-1} at room temperature, which is 29% larger than the reported value. NIH/3T3 mouse fibroblast cell line was used to study the cytotoxicity of the UCNCs with amine surface modifications. The produced UCNCs with surface modification do not impose toxic effect on cells. The findings could help to better apply upconversion nanocubes in bio-imaging by choosing suitable interfacial media.

Introduction

Upconversion nanoparticles can convert excited light with a lower energy into emission light with a higher energy because of the multiphoton excitation-involving nonlinear process, which can be applied in various areas, including luminescent display devices, optical devices, photo-therapy, and medicine, *etc.*[1–4] Most studies indicate that the dopants of lanthanide, such as Er^{3+}, Tm^{3+}, and Ho^{3+}, can produce emission as the optically active centres due to the to the 4f–4f orbital electronic transitions. Fluoride materials, *e.g.* $NaYF_4$ and $NaGdF_4$, normally act as the excellent host lattices because of their high chemical stability and good optical transparency over a wide wavelength range.[5,6] Unique properties of lanthanide-doped upconversion nanomaterials have attracted extensive attention, *e.g.* optical-magnetic bifunctional properties of $NaGdF_4$:Yb^{3+}, Er^{3+}.[7,8] Recently, the effect of shape and surface modification of lanthanide-doped upconversion nanoparticles on their fluorescence properties have been observed.

Various methods have been developed to produce upconversion nanocubes (UCNCs), including hydro(solvo)-thermal reaction, thermal decomposition of rare earth organic precursors, and ionic liquids (ILs) methods.[9–11] Hydro(solvo)-thermal reaction and thermal decomposition can produce highly crystalline and monodispersed nanocubes, while the reactions need highly controlled reaction parameters, *e.g.* temperature, and toxic organic rare earth precursors which bring barriers to further modification for biomedical applications. Whereas, the ionic liquids-related methods yield less uniform nanocubes, but are relatively easy to control the process parameters.[12,13] Therefore, facile synthesis strategies for high-quality UCNCs with controlled composition, crystalline phase, particle size, are highly demanded.[14,15]

On the other hand, studies show that fluorescence properties of upconversion nanoparticles can be affected by energy levers of rare earth ions, the surface modification, *etc.*[16,17] Riman and his co-workers reported that the effects of three different surfactants; trioctylphosphine, polyethylene glycol monooleate, and polyvinylpyrrolidone on the emissions of $NaYF_4$:Yb^{3+}, Er^{3+} nanomaterials.[17] The emission intensity of $NaYF_4$:Yb^{3+}, Er^{3+} dried powder decreases following the order, polyvinylpyrrolidone > polyethylene glycol monooleate > trioctylphosphine > unmodified nanoparticles because of the reduced reflectance loss at the boundary between upconversion nanoparticles with different surfactants and the air. Song *et al.* reported that $NaYF_4$:Yb^{3+}, Er^{3+} nanoparticles modified with thioglycolic acid can transfer hydrophobic upconversion nanoparticles into hydrophilic upconversion nanoparticles, and the results indicate that the blue emission ($^2H_{9/2} \rightarrow {}^4I_{15/2}$) and red emission ($^4F_{9/2} \rightarrow {}^4I_{15/2}$) with respect to the green emission ($^2H_{11/2}$, $^4S_{3/2} \rightarrow {}^4I_{15/2}$) have been enhanced after surface modification.[18] In addition, some studies found that the chelation of

[a]*Department of Chemical and Biochemical Engineering, University of Western Ontario, London, Ontario, N6A 5B9, Canada. E-mail: Jzhang@eng.uwo.ca*

[b]*Department of Medical Biophysics, University of Western Ontario, London, Ontario, N6A 5C1, Canada*

[c]*HORIBA Canada, Inc., 347 Consortium Court, London, ON, N6E 2S8, Canada*

† Electronic supplementary information (ESI) available. See DOI: 10.1039/c7ra03380j

suitable functional group on upconversion nanoparticles can not only affect their morphologies, but lead to the non-radiative relaxation sensitive emission.[16,17,19,20] More efforts are required to understand the environment-sensitive behaviour of UCNCs.

In this paper, we developed a modified solvothermal method to have a one-pot synthesis of $NaGdF_4$:Yb^{3+}, Er^{3+} UCNCs with amine surface modification. It is noted that amine functional group normally increases the hydrophilicity of nanomaterials, and is useful for further conjugating to different molecule. As gadolinium-based upconversion nanomaterials could be used as a dual contrast agent for the magnetic resonance imaging (MRI) and fluorescence imaging.[4,21] The fluorescence and magnetic properties of the UCNCs with surface modification were investigated. The cytotoxicity of the produced UCNCs is also investigated for potential applications in bio-imaging.

Experimental

Materials

All used chemicals including gadolinium(III) nitrate hexahydrate ($Gd(NO_3)_3\cdot 6H_2O$), ytterbium(III) nitrate pentahydrate ($Yb(NO_3)_3\cdot 5H_2O$), erbium(III) nitrate pentahydrate ($Er(NO_3)_3\cdot 5H_2O$), sodium fluoride (NaF), branched polyethylenimine (PEI, $M_w \sim 800$ by LS, average $M_n \sim 600$ by GPC), and ethylene glycol (EG) were purchased from Sigma-Aldrich and used without further purification. Deionized water was used throughout the experiment.

Synthesis of PEI capped $NaGdF_4$:Yb^{3+}, Er^{3+} nanocubes with surface function of amine group

The $NaGdF_4$:Yb^{3+}, Er^{3+} UCNCs were synthesized with a modified solvothermal method.[22] In a typical synthesize process, 1.6 mmol $Gd(NO_3)_3\cdot 6H_2O$, 0.36 mmol $Yb(NO_3)_3\cdot 5H_2O$, 0.38 mmol $Er(NO_3)_3\cdot 5H_2O$, 0.7 g PEI, and 20 mL ethylene glycol were added into a 100 mL three-neck round-bottom flask and dissolved by magnetic stirring. Then, 8 mmol NaF dissolved in 10 mL ethylene glycol were added dropwise into the 100 mL flask. Under reflux, the solution was heated to around 198 °C to keep ethylene glycol boiling for 6 hours under nitrogen gas protection. The as-synthesized upconversion nanocubes were centrifuged and purified with ethanol and water several times, then dried at 60 °C.

Materials characterizations

The size and morphology of UCNCs were characterized by transmission electron microscopy (TEM, Philips CM-10 operated at 80 kV) and high-resolution TEM (FEI Titan 80-300 HB, Gatan 866 model). The UCNCs with surface modification of PEI were identified by Fourier transform infrared (FTIR, Bruker Vector 22 in the range of 600–4500 cm^{-1} with a resolution of 4 cm^{-1} and 64 scans). The crystal structures of UCNCs were studied by X-ray diffraction (XRD, Rigaku rotating-anode X-ray diffractometer with Co-Kα radiation). The fluorescent emission spectrum of $NaGdF_4$:Yb^{3+}, Er^{3+} UCNCs were measured by fluorophotometry (QuantaMsterTM 30, Horiba Canada-PTI) with an external excitation wavelength of 980 nm, 1 W. The aqueous solution was scanned in a cuvette holder while dried sample was scanned in a solid sample holder at 45° degree facing into the excitation source. The magnetic properties of upconversion nanocubes were measured by using a vibrating sample magnetometer (VSM, Lake Shore 7407, moment measure range: 10^{-7} to 10^3 emu; field accuracy: ±0.05% full scale).

Cytotoxicity study

NIH/3T3 mouse fibroblast cells were cultured in flasks with DMEM supplemented with 10% fetal bovine serum (FBS), 100 units per mL penicillin and 100 μg mL^{-1} streptomycin, and 2.5 mg L^{-1} of amphotericin B. Cells were cultivated until 80% confluent or higher and transferred into welled plates. Cells were cultivated in growth media for 24 hours to ensure cell adherence under sterile conditions at 37 °C supplemented with 5% CO_2.

Cell viability with the treatment of the functionalized UCNCs was assessed by using the NIH/3T3 mouse fibroblast cell line from the American Type Culture Collection (ATCC). Approximately 8000 cells were seeded into each well of a 96-well plate and cultivated overnight at 37 °C. NIH/3T3 cells were incubated with 5, 10, 20, and 100 μg mL^{-1} of $NaGdF_4$:Er, Yb UCNCs for 24 hours at 37 °C in triplicate. The cell media was aspirated and rinsed twice with sterile PBS to remove free nanoparticles. Each well was incubated with 200 μL of growth media and 50 μL of sterile 0.5% MTT solution (0.5 mg MTT formazan powder per mL of deionized water) for 4 hours. The media was aspirated and wells were twice rinsed with sterile PBS. 150 μL of DMSO was added to each well to lyse the cells and to dissolve the tetrazolium salt. The absorbance of the plate was measured at 490 nm.

Results and discussion

Materials characterization

TEM and HRTEM were used to characterize the as-synthesized $NaGdF_4$:Yb^{3+}, Er^{3+} UCNCs. Fig. 1a shows the TEM micrograph of highly uniform nanocubes. The average length of the nanocubes is approximately 40 ± 5 nm. Fig. 1b shows the HRTEM image of as-synthesized upconversion nanocubes with highly a crystalline structure. The measured interplanar distance between two adjacent lattice planes was 0.312 nm, corresponding to a (1 1 1) plane of cubic phase $NaGdF_4$ (JCPDS 27-0697).

The XRD profile is shown in Fig. 2. The XRD profile indicates that standard cubic phase (JCPDS 27-0697) dominants in the crystal structures,[23] and the result is compatible with the result of HRTEM. It is also noted that there are two small peaks around 300, which could be caused by the other phase, hexagonal $NaGdF_4$ crystal (JCPDS 27-0699). Compared to the thermal decomposition for producing cubic UCNCs required high temperature, >300 °C,[7,10] the one-pot method utilizing ethylene glycol solution at 198 °C to produce PEI modified UCNCs. In addition, the dopants, *i.e.* Yb^{3+}, and Er^{3+} ions, normally do not change the crystal structures, but may slightly change the lattice strain of the crystals. Therefore, the characteristic peaks of cubic $NaGdF_4$ crystal acting as the host have a slight shift as

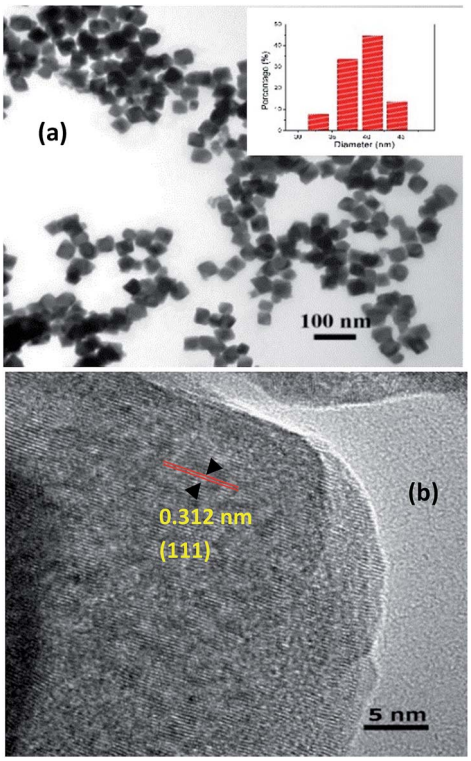

Fig. 1 (a) TEM micrograph of $NaGdF_4$:Yb^{3+}, Er^{3+} UCNCs, the small inset is the size distribution histogram chart. (b) HRTEM image of as-synthesized $NaGdF_4$:Yb^{3+}, Er^{3+} UCNCs.

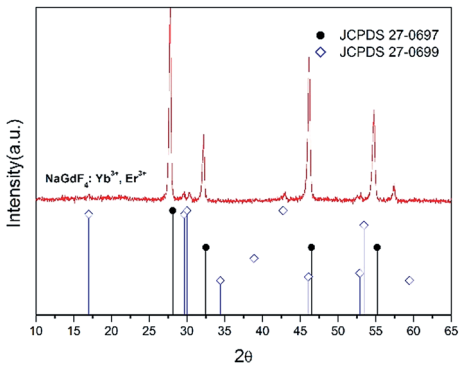

Fig. 2 XRD profile of $NaGdF_4$:Yb^{3+}, Er^{3+} UCNCs and the line pattern of standard cubic phase of $NaGdF_4$ (JCPDS 27-0697) crystal structure.

compared to the standard cubic phase of $NaGdF_4$ (JCPDS 27-0697) crystal structure.

PEI functionalization on the surface of the UCNCs is further investigated by Fourier Transform Infrared (FTIR) spectroscopy. The obtained FTIR spectrum is similar to previous results.[24–26] As shown in Fig. 3, the broad peak at 3300 cm^{-1} is attributed to the –NH– stretching. The small peak at 1640 cm^{-1} is due to the –OC–NH– bending. The peak at 1510 cm^{-1} is the vibration of the amine groups.[27] In addition, the peak at 2300 cm^{-1} 1400 cm^{-1} and can be attributed to the stretching vibrations of $–CH_2–$ and C–C bonds, respectively. These results confirm the successful binding of PEI onto the nanocube surface.

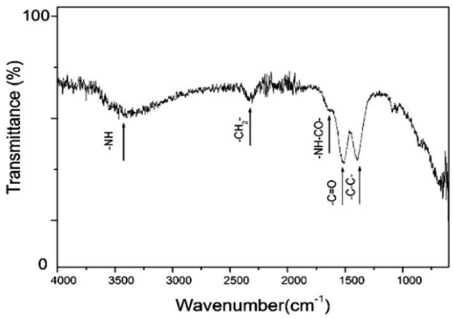

Fig. 3 FTIR spectrum of PEI capped $NaGdF_4$:Yb^{3+}, Er^{3+} UCNCs.

Analysis of upconversion fluorescence

The fluorescence spectra of the UCNCs in both of aqueous solution and dry form are shown in Fig. 4. Under excitation at 980 nm, 1 W, two upconversion emission bands of green light at 540 nm and red light at 660 nm are observed in both of upconversion emission spectra of as-synthesized UCNCs aqueous solution (1 wt%) and dry powder sample (same weight of UCNCs in water). The green light emission ($\lambda_{em} = 540$ nm) is attributed to $^4S_{3/2} \rightarrow {}^4I_{15/2}$ electronic transition, while red light emission ($\lambda_{em} = 660$ nm) is attributed to $^4F_{9/2} \rightarrow {}^4I_{15/2}$ electronic transitions. Emission features of our synthesized UCNCs are comparable to the reported results.[28,29]

In Fig. 4, the emission peaks at 540 nm to both samples show similar value, while the red-light emission peak at 660 nm to dry sample is much more intense than that of UCNCs in aqueous solution. The intensity ratio of red light to green light, $(I_{660}/I_{540})_{aq}$, is 2.49 ± 0.01 to the UCNCs in aqueous solution, while the $(I_{660}/I_{540})_{dry}$ value of UCNCs in dry form is 20.56 ± 0.01. The value of $(I_{660}/I_{540})_{dry}$ is about 8.26 times greater than the value of $(I_{660}/I_{540})_{aq}$.

The difference in the ratio of red light to green light to the aqueous samples and dry sample can be caused by the interaction between water molecules and the PEI modified onto the surface of nanocubes. Aqueous media is likely to decrease the upconversion fluorescence by nonradiative decay. Previous

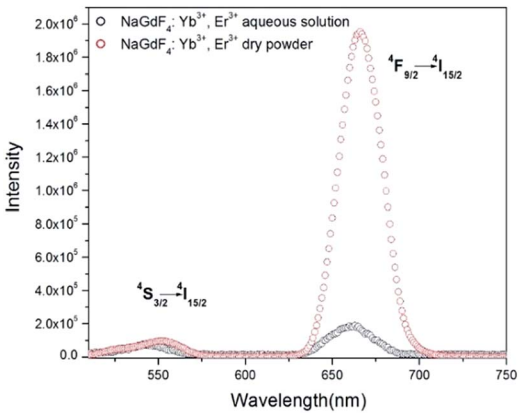

Fig. 4 Upconversion fluorescence spectra of $NaGdF_4$:Yb^{3+}, Er^{3+} UCNCs in deionized water (1 wt%) and dried UCNCs sample under 980 nm, 1 W laser excitation (noted that the as-made UCNCs in the two states have the same weight).

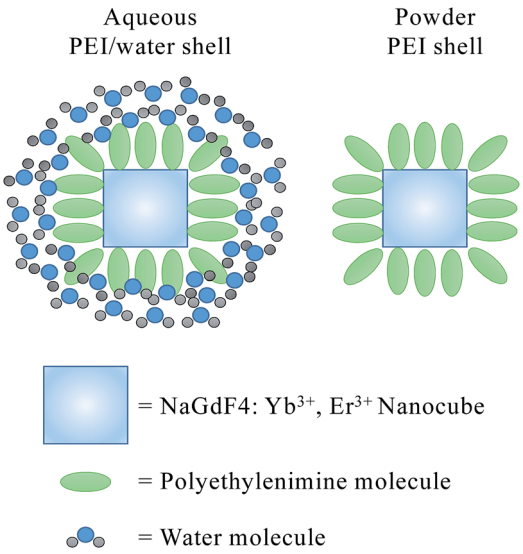

Scheme 1 Schematic of the PEI/water shell on UCNCs in aqueous medium and UCNCs in dry form.

reports indicate that the oleic capped upconversion nanoparticles with a corresponding decrease in luminescence is caused by the nonradiative luminescence decay due to surface binding ligands and water.[30] In our experiment, PEI, a ligand molecule containing many amine groups (–NH–, $-NH_2$), modified on the as-synthesized UCNCs can interact with water molecules through hydrogen bonding.

In addition, we produced $NaGdF_4$:Yb^{3+}, Er^{3+} nanoparticles without PEI by using the same method. Fig. S1† indicates that the ratio $(I_{660}/I_{540})_{dry}$ is 3.067, and the ratio $(I_{660}/I_{540})_{aq}$ is 1.494; the value of $(I_{660}/I_{54})_{dry}$ is about 2.05 times greater than the value of $(I_{660}/I_{540})_{aq}$. Whereas the value of $(I_{660}/I_{540})_{dry}$ is about 8.26 times greater than the value of $(I_{660}/I_{540})_{aq}$ to UCNCs with PEI modification. This results confirm that the interaction between PEI and water molecules enhance the non-radiative relaxation caused by the water absorptivity.

Water molecules surrounding on the nanocube's surface through interacting with PEI results in a dense water shell coated on the nanoparticle surface, which may increase the fluorescence non-radiative decay path. Corresponding schematic is shown in Scheme 1. The cationic polymer molecule of PEI has no light absorption in range of 250 nm to 800 nm.[31] While, the non-radiative relaxation caused by the water absorptivity is sensitive with increasing wavelength, and the red emission is especially sensitive to non-radiative relaxation.[32,33]

Therefore, the PEI/water shell can increase the non-radiative decay path, and leads to a greater decrease of florescence intensity in red light emission ($\lambda_{em} = 660$ nm) than that in green light emission ($\lambda_{em} = 540$ nm).

Magnetic properties analysis

The magnetic properties of as-synthesized $NaGdF_4$:Yb^{3+}, Er^{3+} upconversion nanocubes is measured with a Vibrating Sample Magnetometer (VSM). Fig. 5a shows the hysteresis loop of $NaGdF_4$:Yb^{3+}, Er^{3+} upconversion nanocubes under a magnetic field from 10 kOe to −10 kOe with various temperatures, 85 K, 125 K, 150 K, 200 K, 250 K and 295 K. The UCNCs show typical paramagnetic properties.[34,35]

The magnetic susceptibility (χ) of the UCNCs is calculated by using Curie law;[36]

$$\chi = \frac{M}{H} \quad (1)$$

where M is the magnetization per weight, H the magnetic field. Fig. 5b displays the χ value of the UCNCs as a function of temperature (T), which is a typical curve for paramagnetic materials. At room temperature (295 K), χ value is 1.049×10^{-4} emu g^{-1} Oe^{-1}, which is 29% larger than the reported value of the $NaGdF_4$:Yb^{3+}, Er^{3+} upconversion nanoparticles, $\sim 0.813 \times 10^{-4}$ emu g^{-1} Oe^{-1}.[36,37] It increases with decreasing temperature, when temperature is 85 K, χ value of the UCNCs is 3.361×10^{-4} emu g^{-1} Oe^{-1}, due to thermal fluctuation reduction at low temperatures.[38,39] Reports have indicated that the nanomaterials with higher magnetic susceptibility (χ) can be used for hyperthermia treatments, and contrast agents for MRI imaging.[40] Our produced UCNCs exhibit paramagnetic properties. Therefore, the magnetization (M) normally increases with reducing particle size as reduced particles size normally leads to single domain, or low internal energy barrier.[41] In addition, the

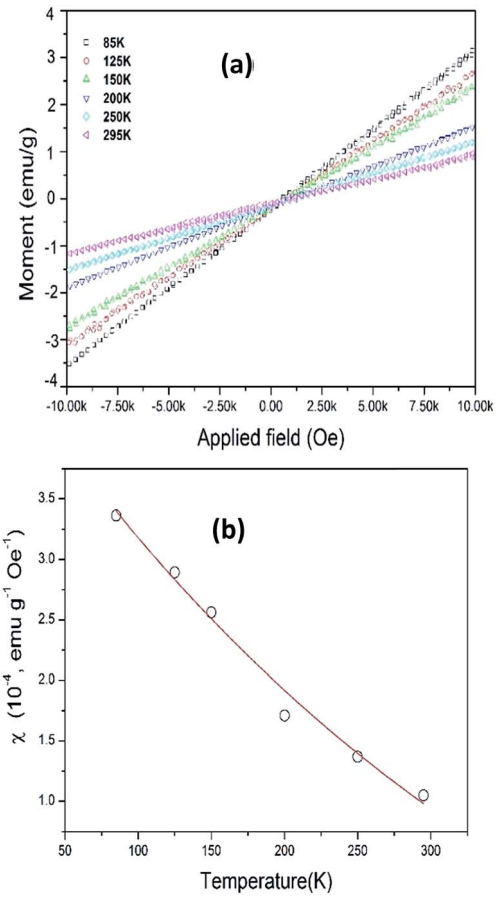

Fig. 5 (a) Magnetic hysteresis curves of PEI capped $NaGdF_4$:Yb^{3+}, Er^{3+} nanocubes with temperatures. (b) $NaGdF_4$:Yb^{3+}, Er^{3+} nanocubes magnetic susceptibility at various temperatures.

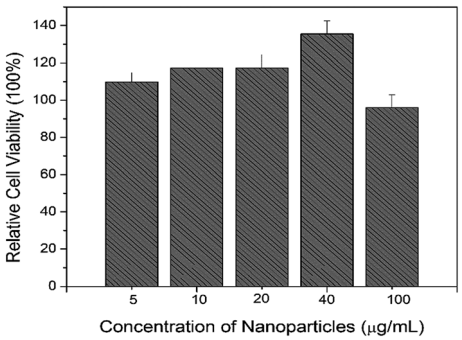

Fig. 6 Relative cell viability as a function of the concentration of UCNCs with surface modification.

cubic structure could allow the nanoparticles having easy magnetization along certain orientation, leading to the reduced magnetic field for saturating UCNCs, $H–H_{anisotropy}$. On the other hand, TEM micrograph (Fig. S2†) shows the $NaGdF_4:Yb^{3+}$, Er^{3+} nanoparticles without PEI have more irregular shape as compared to the UCNCs with PEI, which could result in hard magnetization orientation. Reports have demonstrated that suitable surface modification can result in desired nanostructured in term of uniform particle size, and shape.[42] Thus, the stronger magnetic susceptibility of our produced UCNCs could be related to their cubic structures, the small particle size, and surface modification.

Cytotoxicity study

NIH/3T3 mouse fibroblast cells were used for the cytotoxicity test. The cells without the treatment of UCNCs was used as a control. The relative cell viability of UCNCs with PEI modification are over 110% when the concentration of UCNCs increases from 5 to 40 μg mL^{-1}, it decreases to 97.3% when the concentration of UCNCs increases to 100 μg mL^{-1} as shown in Fig. 6. The relative cell viability for materials with good biocompatibility is normally beyond 85%.[43] Therefore, the as-made UCNCs modified with amine functional group do not impose toxic effect on NIH/3T3 mouse fibroblast cells.

Conclusions

In summary, a facile chemical synthesis method for synthesizing uniform UCNCs with surface modified PEI amine ligands was developed. The as-synthesized $NaGdF_4:Yb^{3+}$, Er^{3+} nanocubes have average length at 40 ± 5 nm, which show good hydrophilicity. The green emission (λ_{em} = 540 nm) and red emission (λ_{em} = 660 nm) can be observed in aqueous solution and dry sample. The upconversion red emissions is intensively strong as compared to the dry sample. The ratio, (I_{660}/I_{540}), of UCNCs in dry form is 8.26 times of that of UCNCs in aqueous solution which could be related to the PEI/water shell. Water absorptivity results in non-radiative decay; and red fluorescent emission is particularly sensitive to non-radiative decay. Moreover, the UCNCs dry sample shows paramagnetic properties with higher magnetic susceptibility of 1.049 × 10^{-4} emu g^{-1} Oe^{-1} at room temperature. In addition, the UCNCs with surface modification do not impose toxic effect on NIH/3T3 mouse fibroblast cell line. The results indicate that such UCNCs can be used as a dual contrast agent in bio-imaging by choosing suitable interfacial media.

Acknowledgements

Authors are thankful for the financial support from Canada Innovation Fund. Tse W. H. is thankful for the Graduate Scholarship offered by the Natural Sciences and Engineering Research Council of Canada (NSERC). Special thanks to Ms. Zahra Farid for assisting on the photoluminescence measurement.

Notes and references

1 F. Auzel, *Chem. Rev.*, 2003, **104**, 139–174.
2 M. Haase and H. Schäfer, *Angew. Chem., Int. Ed.*, 2011, **50**, 5808–5829.
3 S. Heer, K. Kömpe, H. U. Güdel and M. Haase, *Adv. Mater.*, 2004, **16**, 2102–2105.
4 T. H. Shin, Y. S. Choi, S. J. Kim and J. W. Cheon, *Chem. Soc. Rev.*, 2015, **44**, 4501–4516.
5 Z. Li, Y. Zhang and S. Jiang, *Adv. Mater.*, 2008, **20**, 4765–4769.
6 O. S. Kwon, H. S. Song, J. Conde, H. I. Kim, N. Artzi and J. H. Kim, *ACS Nano*, 2016, **10**(1), 1512–1521.
7 J. Liu, W. Bu, L. Pan and J. Shi, *Angew. Chem., Int. Ed.*, 2013, **52**, 4366–4369.
8 G. T. Dai, Z. Q. Zhong, X. F. Wu, S. P. Zhan, S. G. Hu, P. Hu, J. S. Hu, S. B. Wu, J. B. Han and Y. X. Liu, *Nanotechnology*, 2017, **28**, 155702–155707.
9 P. Ramasamy, P. Chandra, S. W. Rhee and J. Kim, *Nanoscale*, 2013, **5**, 8711–8717.
10 W. Niu, S. Wu, S. Zhang, L. T. Su and A. I. Y. Tok, *Nanoscale*, 2013, **5**, 8164–8171.
11 M. He, P. Huang, C. Zhang, F. Chen, C. Wang, J. Ma, R. He and D. Cui, *Chem. Commun.*, 2011, **47**, 9510–9512.
12 N. M. Idris, M. K. G. Jayakumar, A. Bansal and Y. Zhang, *Chem. Soc. Rev.*, 2015, **44**, 1449–1478.
13 G. Chen, H. Qiu, P. N. Prasad and X. Chen, *Chem. Rev.*, 2014, **114**, 5161–5214.
14 W. Feng, C. Han and F. Li, *Adv. Mater.*, 2013, **25**, 5287–5303.
15 G. Wang, Q. Peng and Y. Li, *Acc. Chem. Res.*, 2011, **44**, 322–332.
16 H. J. Wu, Z. W. Yang, J. Y. Liao, S. F. Lai, J. B. Qiu, Z. G. Song, Y. Yang, D. C. Zhou and Z. Y. Yin, *J. Alloys Compd.*, 2014, **586**, 485–487.
17 M. C. Tan, L. Al-Baroudi and R. E. Riman, *ACS Appl. Mater. Interfaces*, 2011, **3**, 3910–3915.
18 D. Li, B. Dong, X. Bai, Y. Wang and H. Song, *J. Phys. Chem. C*, 2010, **114**, 8219–8226.
19 Y. Qu, Y. Yu, X. Kong, Y. Sun, Q. Zeng and H. Zhang, *Mater. Lett.*, 2009, **63**, 1285–1288.
20 J. W. Stouwdam and F. C. J. M. van Veggel, *Langmuir*, 2004, **20**, 11763–11771.

21 M. He, P. Huang, C. Zhang, H. Hu, C. Bao, G. Gao, R. He and D. Cui, *Adv. Funct. Mater.*, 2011, **21**, 4470–4477.
22 H. Wong, M. Tsang, C. Chan, K. Wong, B. Fei and J. Hao, *Nanoscale*, 2013, **5**, 3465–3473.
23 C. Cao, H. K. Yang, J. W. Chung, B. K. Moon, B. C. Choi, J. H. Jeong and K. H. Kim, *J. Mater. Chem.*, 2011, **21**, 10342–10347.
24 J. Chen, C. Guo, M. Wang, L. Huang, L. Wang, C. Mi, J. Li, X. Fang, C. Mao and S. Xu, *J. Mater. Chem.*, 2011, **21**, 2632–2638.
25 Q. Ju, D. Tu, Y. Liu, R. Li, H. Zhu, J. Chen, Z. Chen, M. Huang and X. Chen, *J. Am. Chem. Soc.*, 2012, **134**, 1323–1330.
26 C. F. Chan, M. K. Tsang, H. G. Li, R. F. Lan, F. L. Chadbourne, W. L. Chan, G. L. Law, S. L. Cobb, J. Hao, W. T. Wang and K. L. Wang, *J. Mater. Chem. B*, 2014, **2**, 84–91.
27 J. Zhang, R. Bi, W. Hodge, P. Yin and W. H. Tse, *J. Mater. Chem. B*, 2013, **1**, 4388–4395.
28 F. Li, C. Li, X. Liu, Y. Chen, T. Bai, L. Wang, Z. Shi and S. Feng, *Chem.–Eur. J.*, 2012, **18**, 11641–11646.
29 A. Aebischer, S. Heer, D. Biner, K. Krämer, M. Haase and H. U. Güdel, *Chem. Phys. Lett.*, 2005, **407**, 124–128.
30 R. Naccache, F. Vetrone, V. Mahalingam, L. A. Cuccia and J. A. Capobianco, *Chem. Mater.*, 2009, **21**, 717–723.
31 Z. L. Wang, J. H. Hao and H. L. W. Chan, *J. Mater. Chem.*, 2010, **20**, 3178–3185.
32 W. S. Pegau, D. Gray and J. R. V. Zaneveld, *Appl. Opt.*, 1997, **36**, 6035–6046.
33 V. S. Langford, A. J. McKinley and T. I. Quickenden, *J. Phys. Chem. A*, 2001, **105**, 8916–8921.
34 R. A. J. Litjens, T. I. Quickenden and C. G. Freeman, *Appl. Opt.*, 1999, **38**, 1216–1223.
35 W. Liu, G. Liu, J. Wang, X. Dong and W. Yu, *RSC Adv.*, 2016, **6**, 3250–3258.
36 M. K. Tsang, S. Zeng, H. L. W. Chan and J. Hao, *Opt. Mater.*, 2013, **35**, 2691–2697.
37 Q. Cheng, J. Sui, Y. Li, Z. Zhou and W. Cai, *J. Nanosci. Nanotechnol.*, 2013, **13**, 529–532.
38 R. J. Holmberg, T. Aharen and M. Murugesu, *J. Phys. Chem. Lett.*, 2012, **3**, 3721–3733.
39 G. Gao, C. Zhang, Z. Zhou, X. Zhang, J. Ma, C. Li, W. Jin and D. Cui, *Nanoscale*, 2013, **5**, 351–362.
40 S. Laurent, D. Forge, M. Port, A. Roch, C. Robic, L. V. Elst and R. N. Muller, *Chem. Rev.*, 2008, **108**, 2064–2110.
41 C. Ma, J. Q. Yan, K. W. Dennis, R. W. McCallum and X. Tan, *J. Appl. Phys.*, 2009, **105**, 033908–033913.
42 L. Lei, D. Chen, P. Huang, J. Xu, R. Zhang and Y. S. Wang, *Nanoscale*, 2013, **5**, 11298–11305.
43 R. Mihai, I. P. Florescu, V. Coroiu, A. Oancea and M. Lungu, *J. Med. Life*, 2011, **4**(3), 250–255.